Cation disorder in MgX_2O_4 (X = Al, Ga, In) spinels from first principles

Chao Jiang,[1,*] Kurt E. Sickafus,[2] Christopher R. Stanek,[3] Sven P. Rudin,[4] and Blas P. Uberuaga[3,*]
[1]*State Key Laboratory of Powder Metallurgy, Central South University, Changsha, Hunan 410083, China*
[2]*Department of Materials Science and Engineering, University of Tennessee, Knoxville, Tennessee 37996, USA*
[3]*Materials Science and Technology Division, Los Alamos National Laboratory, Los Alamos, New Mexico 87545, USA*
[4]*Theoretical Division, Los Alamos National Laboratory, Los Alamos, New Mexico 87545, USA*
(Received 29 September 2011; revised manuscript received 11 June 2012; published 23 July 2012)

We have performed first-principles density functional theory calculations to investigate the possible physical origins of the discrepancies between the existing theoretical and experimental studies on cation distribution in MgX_2O_4 (X = Al, Ga, In) spinel oxides. We show that for $MgGa_2O_4$ and $MgIn_2O_4$, it is crucial to consider the effects of lattice vibrations to achieve agreement between theory and experiment. For $MgAl_2O_4$, we find that neglecting short-range order effects in thermodynamic modeling can lead to significant underestimation of the degree of inversion. Furthermore, we demonstrate that the common practice of representing disordered structures by randomly exchanging atoms within a small periodic supercell can incur large computational error due to either insufficient statistical sampling or finite supercell size effects.

DOI: 10.1103/PhysRevB.86.024203 PACS number(s): 61.43.Bn, 05.70.−a, 81.30.Bx, 07.05.Tp

I. INTRODUCTION

Spinel oxides with the general formula AB_2O_4 and space group $Fd\bar{3}m$ form an important class of materials of significant technological and scientific interest.[1] Among them, $MgAl_2O_4$ is considered for application as an inert matrix nuclear fuel due to its excellent radiation damage resistance.[2] $MgIn_2O_4$ is a promising transparent electronic conductor since it possesses both a wide band gap and high electrical conductivity.[3] One fascinating feature of spinel oxides is their ability to accommodate large amounts of cation disorder. In a normal II-III spinel, divalent A^{2+} cations occupy one-eighth of the fourfold-coordinated tetrahedral interstitial sites of the pseudo-face-centered-cubic oxygen sublattice, with trivalent B^{3+} cations occupying half of the sixfold-coordinated octahedral interstices.[4] In many spinels, A and B cations can readily exchange positions with each other, either intrinsically or via thermal excitations or irradiation, giving rise to a wide range of cation distributions with the general formula $(A_{1-x}B_x)_{\text{tet}}(B_{2-x}A_x)_{\text{oct}}O_4$. Here x is the inversion parameter with values ranging between 0 (normal) and 1 (inverse). Precise knowledge of the cation distribution in spinels is critical since many of their fundamental properties depend sensitively on x. For example, our previous studies have shown that cation disorder plays a crucial role in controlling radiation tolerance[2] and defect mobility[5] in spinels. Further, the electronic structures of spinels strongly depend on cation distribution.[6,7]

Numerous theoretical investigations of cation disordering in spinels have been reported in the literature. Wei and Zhang[7] obtained the structural, thermodynamic, and electronic properties of eighteen spinels in both normal and inverse configurations using first-principles local-density-approximation (LDA) calculations. More recently, Seko *et al.*[8,9] predicted the degree of inversion in six II-III spinel oxides using a combination of the cluster expansion (CE) technique and Monte Carlo (MC) simulations. Interestingly, those studies suggest that $MgGa_2O_4$ and $MgIn_2O_4$ behave rather similarly, while the experimentally observed inversion parameter of $MgGa_2O_4$ (x = 0.67,[10] 0.75,[11] 0.81,[12] 0.84–0.90[13]) is noticeably smaller than that of $MgIn_2O_4$ (x = 1.00[10]). By randomly exchanging cations within a 56-atom cubic supercell, Rocha *et al.*[14] obtained the total energy of $MgAl_2O_4$ as a function of inversion. However, their results show large discrepancies (up to 0.17 eV/f.u.) with earlier calculations by Warren *et al.*[15] (see Fig. 1), although rather similar computational procedures were employed in both studies.

In this paper, first-principles calculations are performed to elucidate the origins of the aforementioned discrepancies in the literature. Our study indicates that both lattice vibration and short-range order (SRO) effects can strongly influence the cation distribution in spinels. Furthermore, we show that the usual approach of simulating disordered structures by randomly distributing atoms in a small periodic supercell can incur computational errors due to either insufficient sampling of configurational space or finite supercell size.

II. METHODOLOGY

To reproduce the statistics of randomly disordered inverse and partially inverse spinels as closely as possible in finite supercells, we adopt the special quasirandom structure (SQS) approach.[16–20] Compared with mean-field approaches such as the virtual crystal approximation, the SQS approach has the advantage that local environmentally dependent effects such as charge transfer and local lattice relaxations can be fully taken into account. Using MC simulated annealing,[19,20] we have generated large SQS-N structures (with N atoms per unit cell, $N \geqslant 126$) for spinels with x = 1/2, 2/3, and 1, respectively. For partially inverse spinels, material properties depend on two kinds of interatomic interactions: those between cations within the same sublattice (oct-oct and tet-tet) and the coupling interactions between cations on different sublattices (oct-tet). For inverse spinels, only interactions within the octahedral sublattice need to be considered. As shown in Table I, both the near-neighbor intra- and inter-sublattice pair correlation functions of disordered spinels are accurately reproduced by our SQSs.

TABLE I. Intra-sublattice (oct-oct and tet-tet) and inter-sublattice (oct-tet) pair correlation functions of the SQS structures for mimicking the disordered spinels with various degrees of inversion (nn = nearest neighbor).

		Oct-Oct					Tet-Tet					Oct-Tet		
Inversion	Structure	1nn	2nn	3nn	4nn	5nn	1nn	2nn	3nn	4nn	5nn	1nn	2nn	3nn
$x = 1$	Random	0	0	0	0	0								
	SQS-168	0	0	0	0	0								
$x = 2/3$	Random	0.111	0.111	0.111	0.111	0.111	0.111	0.111	0.111	0.111	0.111	0.111	0.111	0.111
	SQS-126	0.111	0.111	0.111	0.111	0.111	0.111	0.111	0.111	0.111	−0.111	0.111	0.111	0.111
$x = 1/2$	Random	0.25	0.25	0.25	0.25	0.25	0	0	0	0	0	0	0	0
	SQS-168	0.25	0.25	0.25	0.25	0.229	0	0	0	0	−0.111	0	0	0

To evaluate internal energies, we employ the all-electron projector augmented wave method[21] within the LDA, as implemented in VASP.[22] A plane-wave cutoff energy of 500 eV and dense k-point meshes are used to guarantee high numerical accuracy for total energy calculations. The lattice parameters and internal atomic positions of all structures are fully relaxed using a conjugate-gradient scheme. Note that atoms with shallow occupied valence d states (e.g., In and Ga) are known to have a preference for the tetrahedral sites.[7] Thus, we explicitly treat the semicore $4d$ electrons of In and the semicore $3d$ electrons of Ga as valence electrons.

III. RESULTS AND DISCUSSION

Figure 1(a) shows the SQS calculated disordering energies of MgX_2O_4 (X = Al, In, Ga) spinels as a function of x. The disordering energy is defined as the internal energy difference between a disordered spinel with inversion parameter x and a normal spinel, $\Delta E(x) = E(x) - E(0)$. For the sake of comparison with experiments, we have further obtained the effective oxygen displacement parameter u as[4]

$$u = \frac{-11 + 6r^2 + \sqrt{33r^2 - 8}}{24(r^2 - 1)}, \quad (1)$$

where $r = \bar{R}_{oct}/\bar{R}_{tet}$ is the ratio of average tetrahedral and octahedral oxygen-cation bond lengths in our fully relaxed SQSs. In agreement with O'Neill and Navrotsky,[23] our results indicate a strongly nonlinear dependence of the internal energy difference ΔE on the inversion parameter x. For $MgGa_2O_4$ and $MgIn_2O_4$, disordering energies actually exhibit a distinct maximum around $x = 0.5$. In contrast, the effective oxygen displacement parameter u depends almost linearly on x [Fig. 1(b)]. For $MgAl_2O_4$ and $MgGa_2O_4$, the u parameter decreases with increasing inversion, which is consistent with the fact that both Al^{3+} and Ga^{3+} are smaller than Mg^{2+}.[24,25] For $MgIn_2O_4$, the u parameter instead increases with x, which can be explained since In^{3+} is larger than Mg^{2+} (see Table II). Our calculated u parameters for $MgAl_2O_4$ are also in excellent agreement with experimental data.[26,27]

Importantly, Fig. 1(a) shows that the tendency towards cation disordering increases in the order $MgAl_2O_4 < MgIn_2O_4 \approx MgGa_2O_4$. Although this trend agrees rather well with the CE-MC simulations by Seko *et al.*,[9] it would indicate that $MgGa_2O_4$ is even more inverse that $MgIn_2O_4$, which is in apparent contradiction with experiments.

At finite temperatures, instead of considering only $\Delta E(x)$, it is more relevant to consider the change in free energy upon disordering

$$\Delta G(x) = \Delta E(x) - T[\Delta S_c(x) + \Delta S_{nc}(x)], \quad (2)$$

where $\Delta S_c(x)$ and $\Delta S_{nc}(x)$ denote configurational and non-configurational entropy changes on disordering, respectively. It is plausible that non-configurational entropy, which has been neglected in previous first-principles studies, plays an important role in determining the equilibrium cation distribution in spinels. To this end, we have performed phonon calculations on both normal and inverse spinels using density functional perturbation theory (DFPT)[28] within the LDA, as implemented

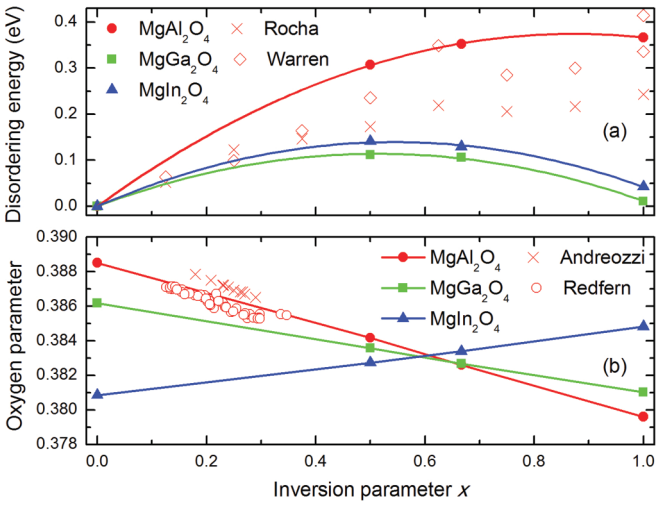

FIG. 1. (Color online) Disordering energies (a) and oxygen parameter (origin at $\bar{4}3m$) (b) of MgX_2O_4 (X = Al, Ga, In) spinels as a function of inversion parameter x. The solid symbols represent present SQS calculations. For $MgAl_2O_4$, results from previous LDA calculations (Refs. 14,15) and experimental measurements (Refs. 26,27) are shown for comparison.

TABLE II. Ionic radii in both tetrahedral and octahedral coordinations from Shannon (Ref. 24).

	Mg^{2+}	Al^{3+}	Ga^{3+}	In^{3+}
Tetrahedral	0.57	0.39	0.47	0.62
Octahedral	0.72	0.535	0.62	0.80

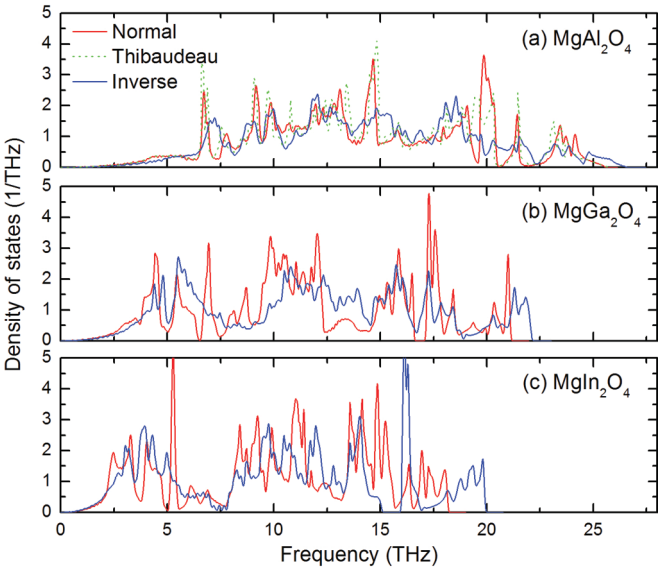

FIG. 2. (Color online) Phonon DOS of (a) $MgAl_2O_4$, (b) $MgGa_2O_4$, and (c) $MgIn_2O_4$ in both normal and inverse states from DFPT calculations. The dotted line denotes the previous calculations by Thibaudeau *et al.* (Ref. 31).

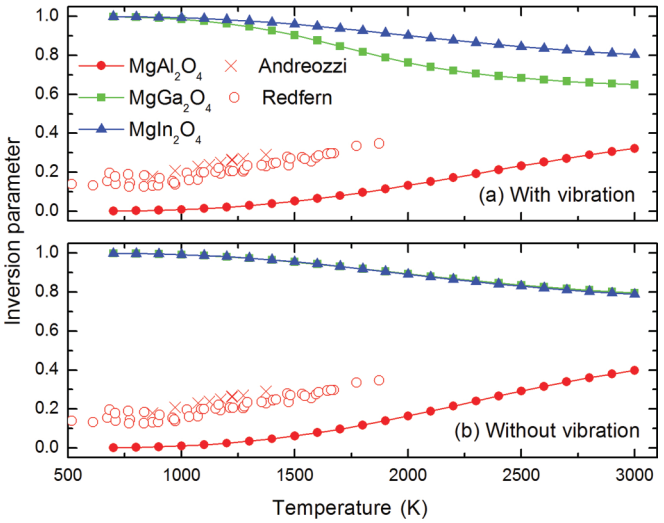

FIG. 3. (Color online) Model calculated equilibrium inversion parameters for MgX_2O_4 (X = Al, Ga, In) spinels, with (a) and without (b) considering the effects of lattice vibrations. For $MgAl_2O_4$, the experimental data from Andreozzi *et al.* (Ref. 26) and Redfern *et al.* (Ref. 27) are shown for comparison.

in ABINIT.[29] For insulators such as $MgAl_2O_4$, $MgGa_2O_4$, and $MgIn_2O_4$, the thermal electronic contribution to the free energy can be neglected. Due to limited computational resources, here we model the inverse spinels using 14-atom SQSs, which have been used in the study of Wei and Zhang.[7] Troullier-Martins pseudopotentials,[30] a plane-wave cutoff energy of 40 Ry, and a $4 \times 4 \times 4$ k-point mesh are employed in our calculations. The interatomic force constants are extracted from a Fourier transform of the dynamical matrices computed on a $4 \times 4 \times 4$ grid in the Brillouin zone.

Figure 2 shows the phonon density of states (DOS) calculated with DFPT and including LO/TO splitting. The DOS of normal and inverse spinels differ significantly due to the drastic change of local coordination of A and B cations. For normal $MgAl_2O_4$, our results are in good agreement with previous calculations by Thibaudeau *et al.*[31] The high-temperature limit of the vibrational entropy difference between the normal and inverse states of a spinel can be directly obtained from a weighted integral of the phonon DOS difference between the two structures as $\Delta S_{\text{vib}} = -k_B \int_0^\infty \ln(\nu) \Delta g(\nu) d\nu$, where ν is the phonon frequency, $g(\nu)$ is the phonon DOS, and k_B is the Boltzmann constant. We calculate ΔS_{vib} to be -0.296, -0.571, and $+0.071$ (in k_B per AB_2O_4 f.u.) for $MgAl_2O_4$, $MgGa_2O_4$, and $MgIn_2O_4$, respectively. For $MgAl_2O_4$, we have also obtained ΔS_{vib} using a larger 28-atom SQS, allowing us to estimate the errors of our calculated ΔS_{vib} using 14-atom SQSs to be about $0.1 k_B$.

For $MgAl_2O_4$, we find ΔS_{vib} to be negative, which is in accordance with the study by Redfern *et al.*[27] For $MgGa_2O_4$ and $MgIn_2O_4$, the values of ΔS_{vib} are of opposite sign. To assess the effects of lattice vibrations on cation distribution, following O'Neill and Navrotsky,[23] we express the disordering energy in Eq. (2) as a quadratic function of x: $\Delta E(x) = ax + bx^2$, with a and b parameters fitted to SQS energetics. $\Delta S_c(x)$ is calculated using the Bragg-Williams approximation:

$$\Delta S_c(x) = -k_B[x \ln(x) + (1-x)\ln(1-x) + x \ln(x/2) + (2-x)\ln(1-x/2)]. \quad (3)$$

For simplicity, we further assume that the non-configurational entropy term can be approximated as $\Delta S_{\text{nc}}(x) = x \Delta S_{\text{vib}}$, that is, as a linear interpolation between the normal and inverse values. The equilibrium inversion parameter at a given temperature can then be calculated through a minimization of $\Delta G(x)$.

Figure 3 shows the predicted equilibrium inversion parameters of MgX_2O_4 (X = Al, Ga, In) spinels with and without the non-configurational entropy term. Indeed, with the incorporation of the effect of lattice vibrations, the equilibrium inversion parameter of $MgGa_2O_4$ becomes considerably less than that of $MgIn_2O_4$. In particular, vibrational entropy drives $MgGa_2O_4$ towards the random ($x = 2/3$) state and $MgIn_2O_4$ slightly towards the inverse state, improving the agreement between theory and experiments for both spinels.

For $MgAl_2O_4$, however, our calculated inversion parameters are significantly lower than experimental data,[26,27] and the agreement is not improved with the inclusion of lattice vibrational effects (Fig. 3). Since such disagreement persists even at high temperatures, it is unlikely due to sluggish kinetics in the experiments. In our SQS calculations, we assume that cations are randomly mixed within their respective sublattices, i.e., no SRO. To assess the validity of such an assumption, we apply the CE[32–36] technique to characterize the dependence of disordering energy on cation arrangement σ in inverse $MgAl_2O_4$:

$$\Delta E_{\text{Inverse}}(\sigma) = J_0 + \sum_f D_f J_f \bar{\Pi}_f(\sigma), \quad (4)$$

where f is a figure composed of a group of k lattice sites ($k = 1, 2, 3$ indicates single site, pair, and triplet, etc.). D_f is the degeneracy factor indicating the number of symmetrically

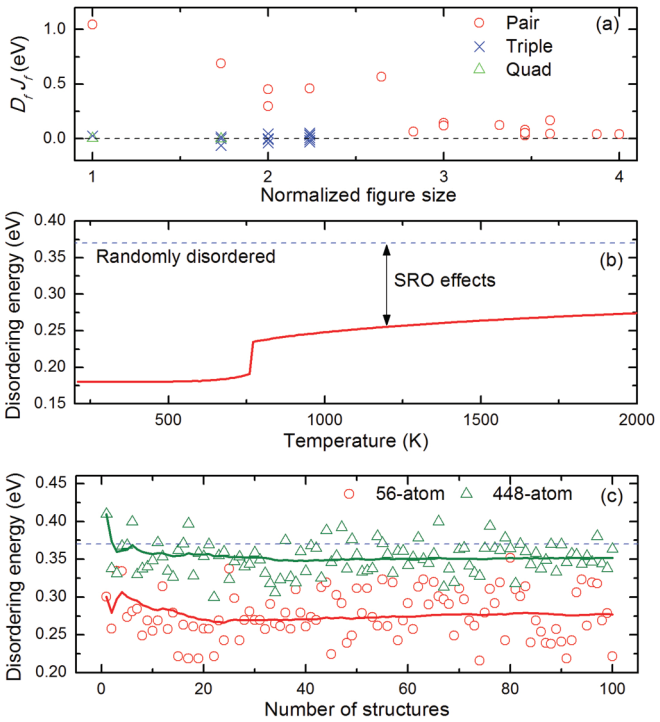

FIG. 4. (Color online) (a) Fitted ECI for cation distribution in the octahedral sublattice in inverse $MgAl_2O_4$. (b) Disordering energy of inverse $MgAl_2O_4$ spinel as a function of temperature from CE-MC simulations. The dashed line denotes the randomly disordered state. (c) Disordering energies of randomly generated inverse $MgAl_2O_4$ configurations. The solid lines denote cumulative moving averages.

equivalent figures of type f per lattice site. J_f is the effective cluster interaction (ECI) for figure f and $\bar{\Pi}_f(\sigma)$ is the correlation function.

We construct a high-fidelity CE by fitting to first-principles-calculated total energies of a set of 146 $MgAl_2O_4$ structures in various inverse configurations. A well-converged CE is obtained using 17 pair, 16 triple, and 2 quadruplet interactions with an average fitting error of only 2.4 meV and a cross-validation score of only 3.4 meV/f.u. Interestingly, we find that the pair interactions are very long ranged and their symmetry-weighted values ($D_f\ J_f$) are nonnegligible even at tenth-nearest neighbor [Fig. 4(a)]. Furthermore, all pair interactions are repulsive ($J_f > 0$) in nature, indicating a tendency towards cation ordering. In comparison, many-body (triple and quadruplet) interactions are much weaker in magnitude. The characteristics of our CE are typical of Coulomb interactions and are consistent with the point-ion electrostatic model of Stevanovic *et al.*[37]

Using our CE, we perform MC simulated annealing simulations in a large $16 \times 16 \times 16$ periodic simulation cell. We start from an extremely high temperature of 100 000 K for a randomly disordered state and slowly cool the system down to lower temperatures. As shown in Fig. 4(b), SRO strongly stabilizes inverse ($x = 1$) $MgAl_2O_4$ at finite temperatures. Even at the highest experimental temperature of 1873 K, we obtain $\Delta E_{\text{Inverse}} = 0.272$ eV/f.u., a 26% reduction from that of the randomly disordered state (0.370 eV/f.u.). Consequently, our SQS calculations, which completely neglect the SRO effects, lead to a considerable overestimation of disordering energies. This overestimation explains why our model calculations, which rely on SQS energetics and the assumption of a fully random cation distribution, consistently underestimate the degree of inversion for $MgAl_2O_4$ [Fig. 3(b)]. Note that when the temperature falls below ~770 K, inverse $MgAl_2O_4$ undergoes a first-order phase transition into a long-range-ordered tetragonal structure with space group $P4_322$, accompanied by a further energy decrease.

Finally, to shed some light on the discrepancies between previous calculations of the disordering energies of $MgAl_2O_4$,[14,15] we have randomly generated 100 inverse $MgAl_2O_4$ configurations by switching Mg with Al atoms within an N-atom cubic supercell of normal $MgAl_2O_4$ with $N = 56$ and 448, respectively. The disordering energies of those structures are then readily evaluated by our CE [Fig. 4(c)]. Indeed, the calculated disordering energies span a large range from 0.216 (0.300) to 0.352 (0.409) eV/f.u. for $N = 56$ (448), suggesting that a single randomly generated configuration is insufficient to adequately represent the disordered state. Such a large variation helps explain the discrepancies between earlier studies.[14,15] By averaging over many randomly generated configurations within each N-atom supercell, the statistical error can be largely eliminated, and the cumulative moving average rapidly converges to a constant value of 0.27 (0.35) eV/f.u. for $N = 56$ (448). Evidently, the statistical error is not the only source of uncertainty in calculating the disorder energy, and finite supercell size itself can also have an effect on the calculated results, which is presumably a consequence of the long-ranged pair interactions in $MgAl_2O_4$.

IV. CONCLUSIONS

To summarize, we have reinvestigated the cation distribution in MgX_2O_4 (X = Al, Ga, In) spinels using first-principles calculations. We find that both lattice vibration and short-range order effects play an important role in determining the equilibrium cation distributions in spinels. It is crucial to take into account both effects in order to reconcile the apparent inconsistencies between theory and experiments. We expect that SRO effects would be strongest for random ($x = 2/3$) spinels as they benefit the most from even limited ordering. While it is straightforward to incorporate the effects of lattice vibrations in thermodynamic modeling, it is necessary to perform Monte Carlo simulations in order to consider the effects of SRO. Concurrently accounting for both key effects and their coupling would necessitate the construction of a temperature-dependent cluster expansion,[38] which is a significant computational challenge for these types of materials.

ACKNOWLEDGMENTS

This work is sponsored by the US Department of Energy (DOE), Office of Basic Energy Sciences (BES), Division of Materials Sciences and Engineering. The work of C.J. is partially supported by the National Natural Science Foundation of China (Grants No. 50901091 and No. 51071180). All calculations are performed using the computing facilities at Los Alamos National Laboratory (LANL).

*Corresponding authors: chaopsu@gmail.com and blas@lanl.gov

[1]X. W. Zhang and A. Zunger, Adv. Funct. Mater. **20**, 1944 (2010).
[2]K. E. Sickafus, A. C. Larson, N. Yu, *et al*., J. Nucl. Mater. **219**, 128 (1995).
[3]N. Ueda, T. Omata, N. Hikuma, *et al*., Appl. Phys. Lett. **61**, 1954 (1992).
[4]K. E. Sickafus, J. M. Wills, and N. W. Grimes, J. Am. Ceram. Soc. **82**, 3279 (1999).
[5]B. P. Uberuaga, D. Bacorisen, R. Simth, J. A. Ball, R. W. Grimes, A. F. Voter, and K. E. Sickafus, Phys. Rev. B **75**, 104116 (2007).
[6]S. D. Mo and W. Y. Ching, Phys. Rev. B **54**, 16555 (1996).
[7]S. H. Wei and S. B. Zhang, Phys. Rev. B **63**, 045112 (2001).
[8]A. Seko, K. Yuge, F. Oba, A. Kuwabara, I. Tanaka, and T. Yamamoto, Phys. Rev. B **73**, 094116 (2006).
[9]A. Seko, K. Yuge, F. Oba, A. Kuwabara, and I. Tanaka, Phys. Rev. B **73**, 184117 (2006).
[10]R. J. Hill, J. R. Craig, and G. V. Gibbs, Phys. Chem. Miner. **4**, 317 (1979).
[11]F. Machatschki, Z. Kristallogr. **82**, 348 (1932).
[12]J. E. Weidenborner, N. R. Stemple, and Y. Okaya, Acta Crystallogr. **20**, 761 (1966).
[13]H. Schmalzried, Z. Phys. Chem. **28**, 203 (1961).
[14]S. D. Rocha and P. Thibaudeau, J. Phys.: Condens. Matter **15**, 7103 (2003).
[15]M. C. Warren, M. T. Dove, and S. A. T. Redfern, J. Phys.: Condens. Matter **12**, L43 (2000).
[16]A. Zunger, S. H. Wei, L. G. Ferreira, and J. E. Bernard, Phys. Rev. Lett. **65**, 353 (1990).
[17]S. H. Wei, L. G. Ferreira, J. E. Bernard, and A. Zunger, Phys. Rev. B **42**, 9622 (1990).
[18]C. Jiang, C. Wolverton, J. Sofo, L. Q. Chen, and Z. K. Liu, Phys. Rev. B **69**, 214202 (2004).
[19]C. Jiang, Acta Mater **57**, 4716 (2009).
[20]C. Jiang, C. R. Stanek, K. E. Sickafus, and B. P. Uberuaga, Phys. Rev. B **79**, 104203 (2009).
[21]G. Kresse and D. Joubert, Phys. Rev. B **59**, 1758 (1999).
[22]G. Kresse and J. Furthmuller, Phys. Rev. B **54**, 11169 (1996).
[23]H. S. C. O'Neill and A. Navrotsky, Am. Mineral. **68**, 181 (1983).
[24]R. D. Shannon, Acta Crystallogr. A **32**, 751 (1976).
[25]As u increases, the oxygen atoms move away from the tetrahedrally coordinated A-site cations along the ⟨111⟩ direction, increasing the volume of tetrahedral interstices at the expense of decreased volume of octahedral interstices.
[26]G. B. Andreozzi, F. Princivalle, H. Skogby, and A. Della Giusta, Am. Mineral. **85**, 1164 (2000).
[27]S. A. T. Redfern, R. J. Harrison, H. S. C. O'Neill, and D. R. R. Wood, Am. Mineral. **84**, 299 (1999).
[28]X. Gonze, D. C. Allan, and M. P. Teter, Phys. Rev. Lett. **68**, 3603 (1992).
[29]X. Gonze, B. Amadon, P. M. Anglade, *et al*., Comput. Phys. Commun. **180**, 2582 (2009).
[30]N. Troullier and J. L. Martins, Phys. Rev. B **43**, 1993 (1991).
[31]P. Thibaudeau, A. Debernardi, V. T. Phuoc, S. da Rocha, and F. Gervais, Phys. Rev. B **73**, 064305 (2006).
[32]J. W. D. Connolly and A. R. Williams, Phys. Rev. B **27**, 5169 (1983).
[33]J. M. Sanchez, F. Ducastelle, and D. Gratias, Physica A **128**, 334 (1984).
[34]C. Wolverton and A. Zunger, Phys. Rev. Lett. **75**, 3162 (1995).
[35]C. Jiang, D. J. Sordelet, and B. Gleeson, Phys. Rev. B **72**, 184203 (2005).
[36]C. Jiang, Phys. Rev. B **78**, 064206 (2008).
[37]V. Stevanovic, M. d'Avezac, and A. Zunger, J. Am. Chem. Soc. **133**, 11649 (2011).
[38]V. Ozolins, C. Wolverton, and A. Zunger, Phys. Rev. B **58**, R5897 (1998).